Ultrasonics 54 (2014) 296–304

Contents lists available at SciVerse ScienceDirect

Ultrasonics

journal homepage: www.elsevier.com/locate/ultras

Fabrication of broadband poly(vinylidene difluoride-trifluroethylene) line-focus ultrasonic transducers for surface acoustic wave measurements of anisotropy of a (100) silicon wafer

Yan Lu [a], Cunfu He [a,*], Guorong Song [a], Bin Wu [a], Cheng-Hsien Chung [b], Yung-Chun Lee [a,b]

[a] College of Mechanical Engineering and Applied Electronics Technology, Beijing University of Technology, Beijing, China
[b] Department of Mechanical Engineering, National Cheng Kung University, Tainan, Taiwan, China

ARTICLE INFO

Article history:
Received 24 December 2012
Received in revised form 10 May 2013
Accepted 4 July 2013
Available online 13 July 2013

Keywords:
Broadband line-focus transducer
P(VDF-TrFE) film
Ferroelectric hysteresis loop
V(*f*,*z*) analysis method
Surface acoustic wave

ABSTRACT

This paper investigates a new method for fabrication of broadband line-focus ultrasonic transducers by sol–gel spin-coating the poly(vinylidene difluoride-trifluroethylene) [P(VDF-TrFE)] copolymer film on a concave fine-polished beryllium copper backing. The ferroelectric hysteresis loops of the P(VDF-TrFE) films spin-coated from different molar ratios of VDF/TrFE, 77/23 and 55/45, were measured to select the better mixture. Owing to the better acoustic matching to water, compared with lead zirconate titanate (PZT), the fabricated transducers show relatively wide bandwidth of approximately 50 MHz with high central frequency of 60 MHz obtained at the focal plane when a fused-quartz acts as a reflecting target. Each one of the two finished transducers has a focal length of 5 mm and a full aperture angle of 90°. After applying the specially developed digital signal processing algorithm to the defocusing experiment data, which is called *V*(*f*,*z*) analysis method based on two-dimensional fast Fourier transform (2-D FFT), the operating frequency can extend from several MHz to over 90 MHz. Surface acoustic wave (SAW) velocities of a typical (100) silicon wafer was measured along various directions between [100] and [010] to represent the anisotropic features.

1. Introduction

Material characterization by ultrasound techniques plays a vital role in nondestructive evaluations. Acoustic microscopy (AM) and laser ultrasound system (LUS) are mainly applied for non-contact measurements. However, for AM an immersion medium like water is commonly necessary. Usually, the LUSs [1–3] are very complicated and expensive, in which a separated interferometer should be employed as a detector. While high power laser is used to improve its generation efficiency and sensitivity, additional safety precautions are required. Compared with the LUSs, quantitative material characterization by acoustic microscopy has become a widespread technique for the nondestructive evaluation. After Lemons and Quate [4] developed the first AM as a scanning version, Atalar et al. [5] were the first to monitor the amplitude of the transducer output voltage *V* as a function of spacing *z* from specimen toward lens, or the *V*(*z*) curve. They found that the *V*(*z*) curve has a characteristic response which is dependent upon the elastic properties of the reflecting surface. Later, Weglein and Wilson [6] reported on the periodicity of dips appearing in *V*(*z*) curves. Parmon and Bertoni [7] yielded a clear physical picture of signal formation in the reflection acoustic microscope and provided a simple formula for determining the SAW velocity from acoustic microscopy measurements. The next move toward quantitative measurements of anisotropic materials was taken by Kushibiki and colleagues [8] who invented the line-focus-beam (LFB) technique by means of measuring the interference phenomena in *V*(*z*) curves.

Different from point-focus transducers [9,10], the line-focus ones can generate directional surface waves propagating perpendicularly to the focus line, so that it can be used for material anisotropy and stress determination [11–13]. As shown in [4,8,14,15], the traditional design, using sapphire or quartz to focus the transmitted signals, has to afford significant energy loss at the lens/water interface. In order to reduce the energy loss, a matching layer may be applied on the interface, but the result still did not meet the expectations. Generally, the conventional transducers are of narrowband type, and most of the time they work under radio-frequency tone-burst conditions which are difficult for consecutive phase velocity tracing in wideband measurements.

Piezoelectric copolymers have become more and more popular in fabrication of ultrasound transducers. Its mechanical flexibility, favorable ferroelectricity and relatively low acoustic impedance can abandon the matching layer or the focusing lens. Basically, the fabrication approaches based on polymer films can be divided

* Corresponding author. Tel.: +86 13811788182.
E-mail address: cunfuhe@gmail.com (C. He).

0041-624X/$ - see front matter © 2013 Elsevier B.V. All rights reserved.
http://dx.doi.org/10.1016/j.ultras.2013.07.006

broadly into two classes, viz., to permanently bend a commercial piezoelectric polymer onto a concave cylindrical or spherical backing [10,11,16,17], and to form a piezoelectric polymer onto the concave backing by sol–gel spin-coating process [18–21]. The commercially available PVDF or P(VDF-TrFE) films are typically beyond 10 μm. Specially for PVDF films, it has to be stretched during polarization [19]. Besides, the polarized P(VDF-TrFE) films possess a stronger piezoelectricity than that of PVDF [18]. According to the absence of stretching force while poling, it will be easy to pole the P(VDF-TrFE) films coated on concave surfaces. Therefore, spin-coating a P(VDF-TrFE) copolymer film from its solution onto the prepared backings is a better way to fabricate high frequency and/or large aperture transducers. However, Kimura and Ohigashi [18] did not show how to fabricate the P(VDF-TrFE) focusing transducers in details, and unfortunately the effective area of the active element was only 1.8 mm^2. Robert [19] constructed a point focus transducer with an aluminum backing which is harder to be polished compared with stainless steel or tungsten carbide. But according to its higher f_N number (ratio of focal length to aperture length) in contrast with those transducers applied in material characterization [22,23], it was the relatively small aperture that set a limitation to the application range, in other words, there were barely possibilities to generate guided waves propagating on the specimen. This paper extends the sol–gel spin-coating method involved in Chung's work [21], and improves the approach so that it can be achieved on a line-focus transducer. Finally, two plane type P(VDF-TrFE) films are formed to demonstrate the ferroelectric hysteresis loops, so as to select the better molar ratios of VDF/TrFE between 77/23 and 55/45. Two line-focus type transducers are developed based on this new fabrication procedure. One is fabricated, to some extent, according to Robert's "solvent-evaporated first, film-crystalized second" principle [19] for comparison, but in which only one film layer was made; the other is constructed by the new means of the improved "spin-coating thermal-crystallization simultaneously" one-process method.

The finished transducer will be applied in a defocusing measurement of a (100)-oriented silicon wafer to demonstrate the anisotropy between [100] and [010] directions in terms of the leaky SAW velocities. There are basically two approaches to analyze the defocus-measuring data: (1) time-resolved technique [11,12]; (2) $V(f,z)$ analysis method [22–25] based on $V(z)$ curves measurements [8,26,27]. The former one needs to calculate the delay time Δt between the normally incident waves and the leaky SAW, which are separated gradually during defocus measurements. Δt will be proportional to the defocusing interval Δz_{in}. In this way, one can determine the Rayleigh surface wave velocity from the ratio of $\Delta t/\Delta z_{in}$. However, it can only be realized in non-dispersive surface wave measurements. To solve this problem, Yang [28] proposed a $V(f,z)$ waveform processing method where f and z are frequency and defocus distance respectively. This method records every waveform at different defocusing positions. After Fourier transforms the time domain to frequency domain, at each single f, the curve of normalized amplitude versus z seems like the well-known $V(z)$ curves. In order to extract the oscillation period Δz, secondly Fourier transforms the defocus distance to wave number or $1/z$ domain stemming from the conventional AM [29,30]. Using this $V(f,z)$ analysis method based on 2-D FFT [31], the working frequency can extend from several MHz to over 90 MHz. The obtained results of the leaky SAW velocities are in good agreement with the theoretical data calculated through the method reported in Ref. [32].

2. Line-focus transducer fabrication

The transducer design principles, ferroelectric hysteresis loops and the modified fabrication process will be demonstrated in this section. The methods we introduced herein are meant to establish a feasible approach for broadband line-focus transducer constructions.

2.1. Design principles

The transducers are specially designed for material characterization, i.e. generating Rayleigh waves and/or Lamb waves on the sample. Due to the impedance close to water, the P(VDF-TrFE) films are expected to show narrow impulse response without ring down in time-domain and hence have a large bandwidth. There are three parameters that constrain the performance of the focusing transducers, viz., P(VDF-TrFE) film thickness, full aperture angle (2θ) and focusing radius (R). Fig. 1 shows a brief configuration of the P(VDF-TrFE) line-focus transducer. Film thickness plays an important role in the resonance spectrum, and the formation of the film will be addressed in Section 2.3.

For $V(f,z)$ measurements, the aperture angle and focusing radius are the vital considerations. The aperture angle should cover the critical angle of the specimen so as to emit guided waves, e.g., Rayleigh waves generated at Rayleigh angle which can be determined by the Snell's law:

$$\frac{v_w}{\sin(\theta_w)} = \frac{v_R}{\sin(90^\circ)} \tag{1}$$

where v_w is the water velocity, θ_w is the critical incident angle, v_R is the Rayleigh wave speed. In order to induce the Rayleigh wave successfully, the aperture angle of the transducer should be larger than the critical incident angle, and then an full aperture angle of $2\theta = 90^\circ$ is accepted on purpose to cover the low-SAW-velocity materials.

The curvature radius is governed by the following equation [8]:

$$v_{RL}(f) = v_w\left[1 - \left(1 - \frac{v_w}{2\cdot f\cdot \Delta z}\right)^2\right]^{-1/2} \tag{2}$$

where f is the exciting frequency, Δz is the oscillation period. While v_{RL} is a given value, we can draw the relationship between oscillation period Δz and the exciting frequency f, as shown in Fig. 2.

According to the past experience [19–21], the center frequency of point-focus transducer tend to be around 50 MHz using spin-coating method. Here we assume that our line-focus transducers are at least in par if not better than those mentioned. The Rayleigh wave speed of commonly used materials is below 6000 m/s. Hence, the point A on the solid line in Fig. 2 indicates a oscillation period of 0.47 mm. However, accurately measuring the oscillation period requires several oscillations, usually 5–10. Considering that the wave attenuation in water is proportional to the square of frequency, here 7 oscillations are used in the defocusing distance. Taking the full aperture angle into account, the curvature radius is $\sqrt{2}$ times that of defocusing distance. The focus radius ought to be $0.47 \times 7 \times \sqrt{2} = 4.65$ mm. Furthermore, it should be noted that the defocusing distance is limited by the transducer geometry (the endpiece of the brass holder in Fig. 1), which means less than $R\cdot cos\theta$. Finally, the focus radius of 5 mm is adopted.

2.2. Preparation

Beryllium copper backings are adopted in this work for certain reasons. Different from the press-made smooth concave surface on aluminum substrate, beryllium copper is not so hard as stainless steel and is preferable to be fine polished. Its melting point of around 900 °C can afford the film crystallization temperature, and its relatively low coefficient of thermal expansion will not lead to wrinkles on the film. The conventional method of press-made aluminum backings often induce a macroscopic bend versus the

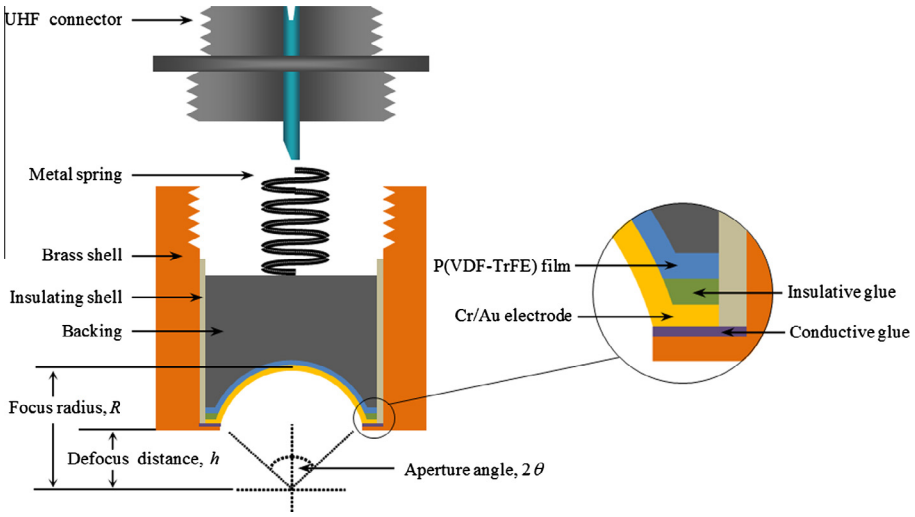

Fig. 1. Schematic cross section of P(VDF-TrFE) line-focus transducer.

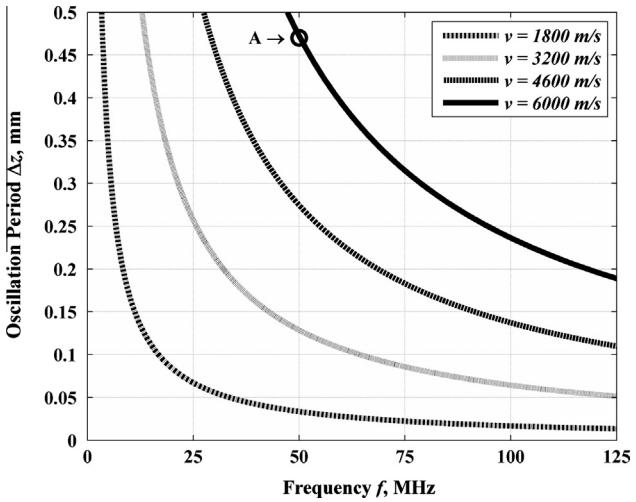

Fig. 2. Relationship between oscillation period and exciting frequency.

axis of the cylinder backing, which will negatively affect the distribution of the acoustic field and the uniformity of the spin-coated P(VDF-TrFE) films. The first step to obtain the smooth surface is to form a desired cylindrical surface by a ultrahigh speed milling machine on top of a beryllium copper cylinder which has a diameter of 10 mm. Secondly, the formed surface is sanded to reduce the chatter marks. Finally, the backing is cylindrically grinded to mirror class (the average roughness is around 10 nm) with great care to maintain the geometry size. If there are scratches on the surface, polarization is difficult because of they cause local discharges.

Two types of solutions were prepared: (1) 9 g P(VDF-TrFE) copolymer powder (Piezotech, France) with a 77/23 molar ratio was dissolved in 30 ml dimethyl formamide (DMF, Fluka, Japan) solvent to make Solution A; (2) 9 g P(VDF-TrFE) copolymer powder with a 55/45 molar ratio was dissolved in 30 ml DMF solvent to make Solution B. Solution A and B are refluxed at 60 °C to be completely dissolved, and then both of them hold on at 50 °C for 5 h to promote the homogeneity. Afterwards, keep them in a moisture-proof cabinet at room temperature. It will be preserved for months.

The finished solution A seems thicker than solution B. This may be due to the molecular weight of TrFE is larger than VDF, so that at the same grams P(VDF-TrFE) copolymer of 77/23 has more molecules than that of 55/45.

2.3. Films fabrication and characterization

Two plane type P(VDF-TrFE) films made from solution A and B respectively are used to analyze their performance in ferroelectric hysteresis loops, so that one can determine which solution should be selected on the concave type. The plane type and the concave type films are formed through exactly the same processing procedures, which is the new method as shown in Fig. 3. Though the new backing has a low roughness, there still exists two sharp straight line edges lying at the intersection of the top flat surface and the concave surface. Chung [21] merged the spin-coating and thermal-curing processes into one by heating up the film while keeping the spinning, the thermal-curing process was still divided into two stages. A 1 min period without thermal heating was performed while spin-coating the solution, and then a lamp started to heat up the film in the following 4 min time while keeping the spinning. Strictly speaking, this is still the "solvent-evaporated first, film-crystalized second" principle, only maintaining spinning while crystallization. More important is that the first stage will lead to film delamination at the sharp line edges. Another problem is that it is very difficult for the smoother concave surface with lower roughness to grab the solution while spinning with a high rate. Furthermore, while spinning, the centrifugal force on a cylindrical surface is not as uniform as a spherical surface. To solve these difficulties, the spun solution should be solidified to film as soon as possible. So the backings were heated up to 70 °C before spinning, and the 1 min solvent-evaporating period was omitted.

As shown in Fig. 3, after the backing or silicon wafer was centered on the vacuum chuck of the spin coater (Laurell Technologies Inc. USA), a big blob of P(VDF-TrFE) solution was dropped on the backing or wafer to cover the whole top surface, then put a high power lamp on the spin coater and a thermometer was inserted nearby the backing or wafer. A spinning rate of 5000 rpm was applied simultaneously with the thermal heating. The temperature was controlled between 120 °C and 140 °C to enhance the crystallinity. 3 min later, the backing or wafer was moved to a hot plate of 70 °C for 30 min, then cooled down to room temperature.

Several factors contribute to the quality of the film: the ratio of VDF to TrFE, the film thickness, and the ferroelectric properties. Two plane type films were made on silicon by the new method to explore these factors. Film A and B are formed from the Solution

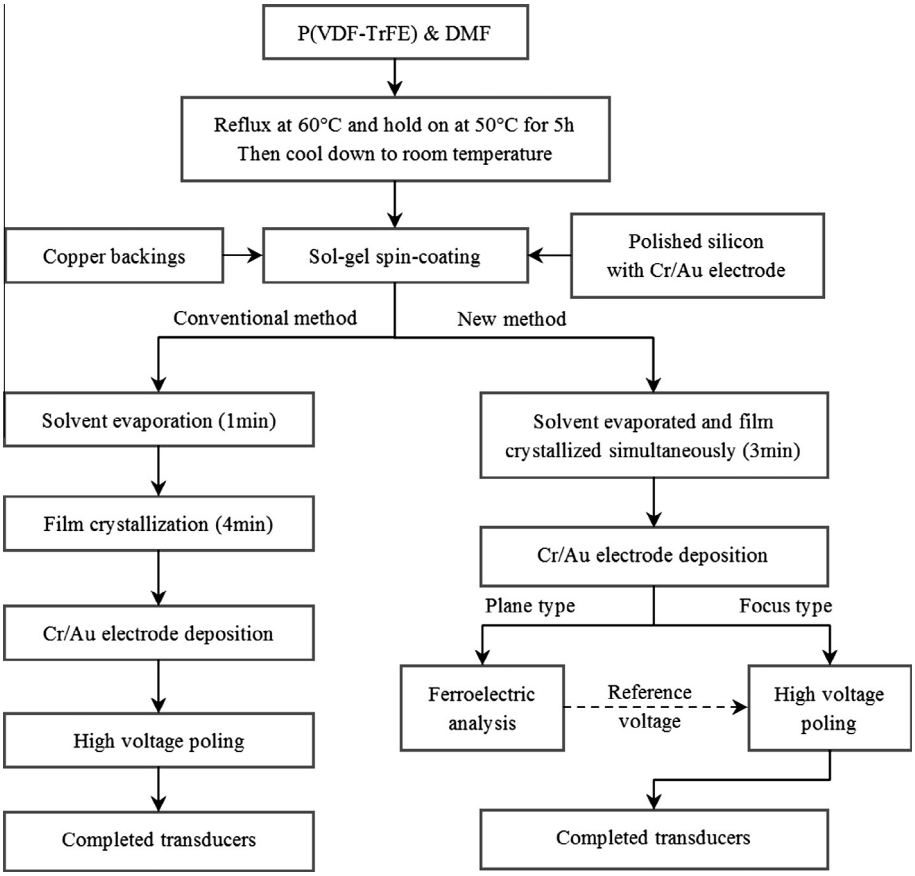

Fig. 3. Flow chart of the fabrication of line-focus P(VDF-TrFE) transducers.

A and B respectively. Circular top electrodes of Au/Cr with a diameter of 1 mm were evaporated through a mask onto Film A and B. Then the ferroelectric hysteresis loops were measured by a ferroelectric analyzer (Radiant Technologies, USA) with a high voltage amplifier (Model 609E-6, Trek, USA). In order to make sure of the film thickness and to change the voltage axis to electric field axis, scanning electron microscopy (SEM, S-3000H, Hitachi, Japan) images of the cross section of Film A and B were brought out to measure the film thickness. All the results are shown in Figs. 4 and 5 respectively.

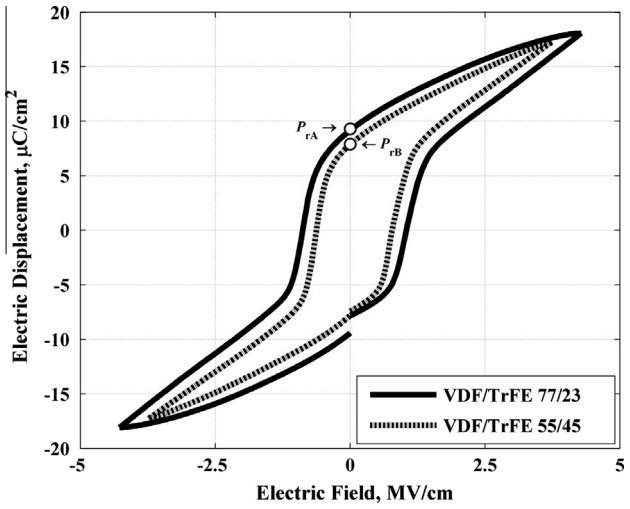

Fig. 4. Ferroelectric hysteresis loops of P(VDF-TrFE) films with different molar ratio at the same maximum poling voltage of 3000 V.

As shown in Fig. 5, the cross section SEM images of Film A and B with VDF/TrFE molar ratio of 77/23 and 55/45 represent that the thickness are 7–8 μm. In Fig. 4, the measured hysteresis loops indicate that, under the same maximum poling voltage of 3000 V, the remanent polarization of Film A (the outer solid line) has a higher value of $P_{rA} = 9.17\ \mu C/cm^2$, which means better piezoelectric features, while Film B (the inner dashed line) $P_{rB} = 7.87\ \mu C/cm^2$. However, the copolymer film of 55/45 is difficult to be polarized with a large active area [33]. Consequently, Solution A with VDF/TrFE molar ratio of 77/23 was selected to construct the line-focus transducers.

2.4. Transducer fabrication and characterization

Two line-focus transducers (namely LT1 and LT2) were finally fabricated with Solution A: (1) LT1 was exactly through the new method mentioned in Section 2.3; (2) LT2 was made by the conventional method, in which 40 s time period was for the solvent evaporation and 2min20s for the thermal crystallization while spinning, and the rest of the procedures are the same as the new method. After several trials on poling our transducers, we found that the challenge is to polarize homogeneously without local discharge and breakdown. Because of the 5 mm focal radius and the 90° full angle, the poling voltage was limited to a maximum voltage of 500 V using a high voltage DC power supply (Matsusada Precision, Japan). The voltage was increasing gradually in a step of 50 V per 15 s to reach the final poling voltage, and poling at the maximum voltage for at least 3 h. Both LT1 and LT2 were polarized by the same poling strategy.

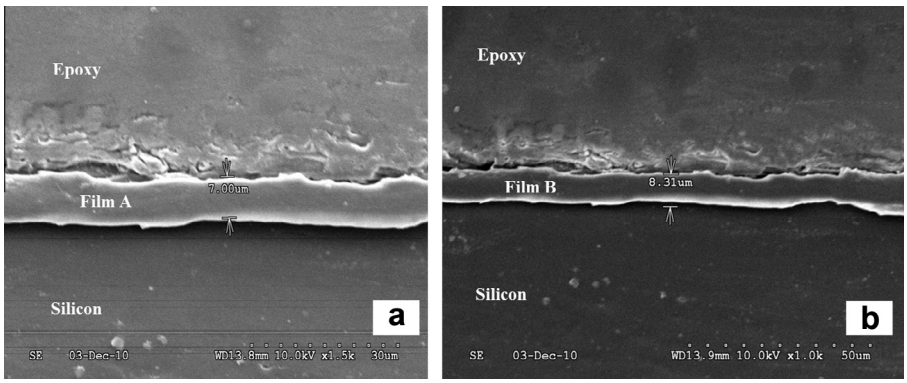

Fig. 5. SEM observations of P(VDF-TrFE) film thickness with different molar ratio of: (a) 77/23, and (b) 55/45.

Both of the transducers (LT1 and LT2) were characterized by standard pulse-echo experiments. As shown in Fig. 6, the system consists of a line-focus transducer, a pulser/receiver (PR5900, Olympus, USA), a digital oscilloscope (TDS3032B, Tektronix, USA), an embedded system (PXI-8110, National Instruments, USA), a motion controller (PXI-7340, National Instruments, USA), multi-axis motion drivers, a linear stage and a rotation stage. A fused-quartz wafer was utilized as a reflector, which was submerged in a tank filled with water as the coupling fluid and placed at the focal plane of the transducer. The pulser/receiver exited the transducer to emit a broadband pulse acoustic wave, and the reflected signal was recorded by the oscilloscope and was stored in the system via a GPIB interface. Typical pulse-echo signals and their spectrum are demonstrated in Fig. 7.

The typical pulse-echo tests were performed under the same experimental settings in pulser/receiver: 1 μJ energy, 50 Ω damping, 3–100 MHz band-pass filter and 40 dB gain. Fig. 7(a) shows that LT1 fabricated with the new method exhibits a very high center frequency of 60 MHz and its −6 dB bandwidth of the spectrum reaches 50 MHz, while LT2 from the conventional method only has a center frequency of approximately 43 MHz with a −6 dB bandwidth of 30 MHz, as shown in Fig. 7(b). Obviously, the improved "spin-coating thermal-crystallization simultaneously" one-process method can be applied to make high quality P(VDF-TrFE) films, and high-frequency broadband line-focus transducers in better performance. Moreover, this method possess wide applicability that it can be totally applied on the fabrication of point-focus transducers. The details of the transducers are listed in Table 1.

3. Measurements of anisotropy of a (100) silicon wafer

Line-focus transducers can be applied on mechanical characterization for both isotropic and anisotropic materials. Fig. 6 shows schematically the $V(f,z)$ defocusing measurement system, in which transducer LT1 will be applied on measuring the leaky SAW velocities of a (100)-oriented silicon wafer to demonstrate the anisotropy between [100] and [010] directions.

3.1. V(f,z) measurements principles

The $V(f,z)$ measurements principles are very similar to the well-known time-resolved technique, which is firstly developed by Hsu's group [11,12]. In defocusing conditions, the defocusing distance z is the space between the focal plane and the specimen top surface, as shown in Fig. 6. The pulser/receiver excites the transducer to emit a pulsed acoustic wave, which will be reflected to the transducer in terms of ray #1 (direct wave) and ray #2 (surface wave). As the transducer moves towards the specimen, ray #1 and ray #2 will separate clearly. Finally, we will obtain a series of waveforms at different defocusing distance. The time

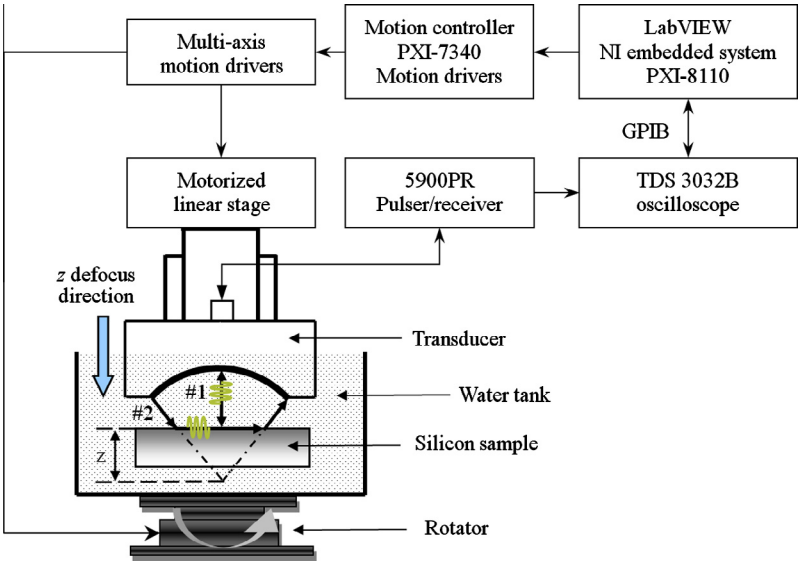

Fig. 6. Pulse-echo/defocusing measurement system.

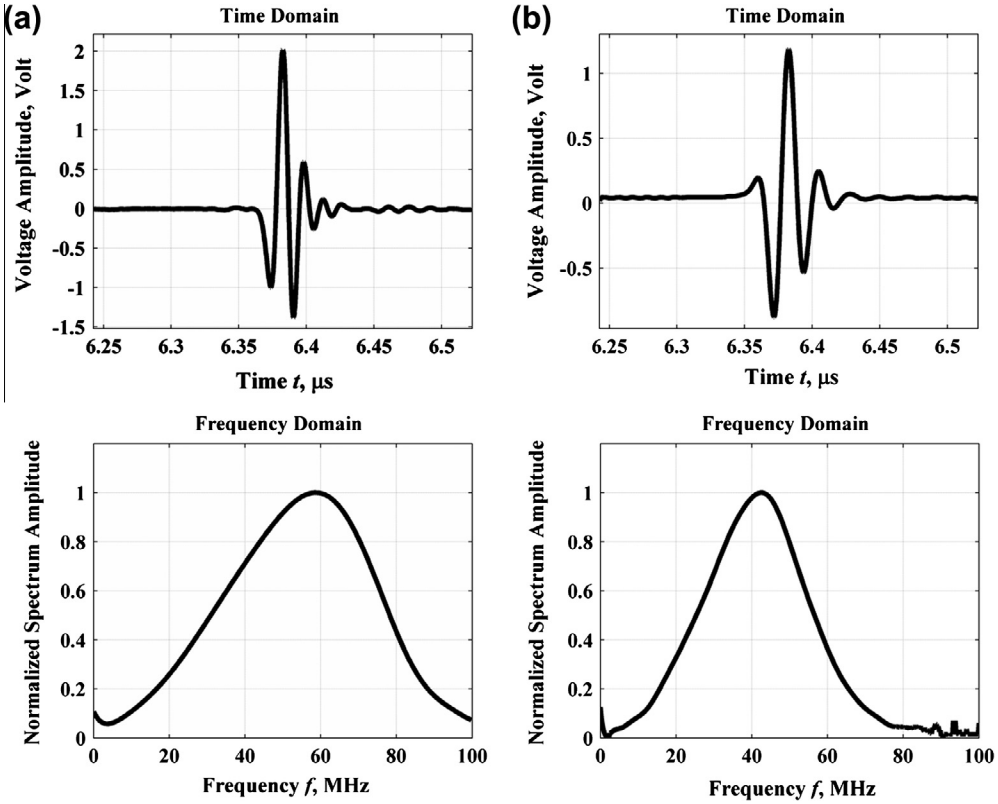

Fig. 7. Pulse-echo response both in time and frequency domain at the focal plane: (a) LT1 with new method, (b) LT2 with conventional method.

Table 1
Specifications of fabricated P(VDF-TrFE) line-focus transducers.

	LT1	LT2
Full aperture angle	90°	90°
Focal radius	5 mm	5 mm
Defocus distance	2 mm	2 mm
Center frequency	60 MHz	43 MHz
−6 dB bandwidth	50 MHz	30 MHz

delay Δt between ray #1 and ray #2 is proportional to defocusing distance z. Once the slope is determined, $m = \Delta t/z$, the leaky surface wave velocities v_{SAW} are given by [11,12]:

$$v_{SAW} = v_w\left[1 - \left(1 - \frac{m \cdot v_w}{2}\right)^2\right]^{-1/2} \quad (3)$$

Though Eq. (2) looks similar to Eq. (3), they differ because Eq. (2) holds for tone-burst excitation while Eq. (3) holds for broadband pulse excitation. If one can perform a broadband defocusing measurement using time-resolved technique and determine every Δz at every single frequency included in the bandwidth, a series of consecutive surface wave velocities are obtained by Eq. (2). In this way, by averaging the non-dispersive surface velocities the measurement accuracy will be greatly improved.

Lee's group [22,34] explored the underlying principles of this $V(f,z)$ measurement by a 2-D FFT waveform processing method, and applied it on the dispersion curves of thin plates. Firstly, assuming that A(t) is the time history of the transient wave function, the directly reflected signal ray #1 can be represented as $A_0(t)$, and for a non-dispersive case the ray #2 can be noted as $a(z) \cdot A_0(t - mz)$. Here, $a(z)$ is an amplitude factor as a function of defocusing distance z, and m is the ratio of time delay at different z. Also, for a non-dispersive measurement m is a constant. Consequently we can get the waveform representation in terms of t and z:

$$A(t,z) = A_0(t) + a(z) \cdot A_0(t - mz) \quad (4)$$

Fourier transform Eq. (4) to frequency domain:

$$V(f,z) = V_0(f) + a(z) \cdot V_0(f) \cdot e^{j\cdot 2\pi f \cdot mz} \quad (5)$$

For a fixed frequency f, the amplitude $|V(f,z)|$ is a periodic function of z, and the oscillating period ought to be written as:

$$\Delta z = (f \cdot m)^{-1} \quad (6)$$

Substitute Eq. (6) into Eq. (3), we can get the same equation as Eq. (2). Thus, the connection between time-resolved technique and the $V(f,z)$ method is derived for non-dispersive wave measurement.

3.2. V(f,z) measurements on a (100) silicon

A 500 μm thick (100) Si wafer was used as a target. The defocus measurements covered 0–90° from [100] to [010] direction with an interval of 2°. Actually, in order to simplify the theoretical calculation, the measurements started from [100]+0.5° direction. At every azimuthal direction, the defocusing distance and interval are 1.2 mm and 10 μm respectively. The entire motion control, waveform measurement and data acquisition are carried out automatically by an integrated LabVIEW (National Instruments, USA) program. It should be mentioned that, each of the waveforms will be shifted in time domain so that the arrival time of the ray #1 echo is coincident to the original time reference. And the waveform amplitudes will be normalized with respect to the magnitude of the ray #1. To demonstrate the $V(f,z)$ waveform processing method in image style, as follows in Fig. 8, a selected series of waveforms from 10.5° will be used.

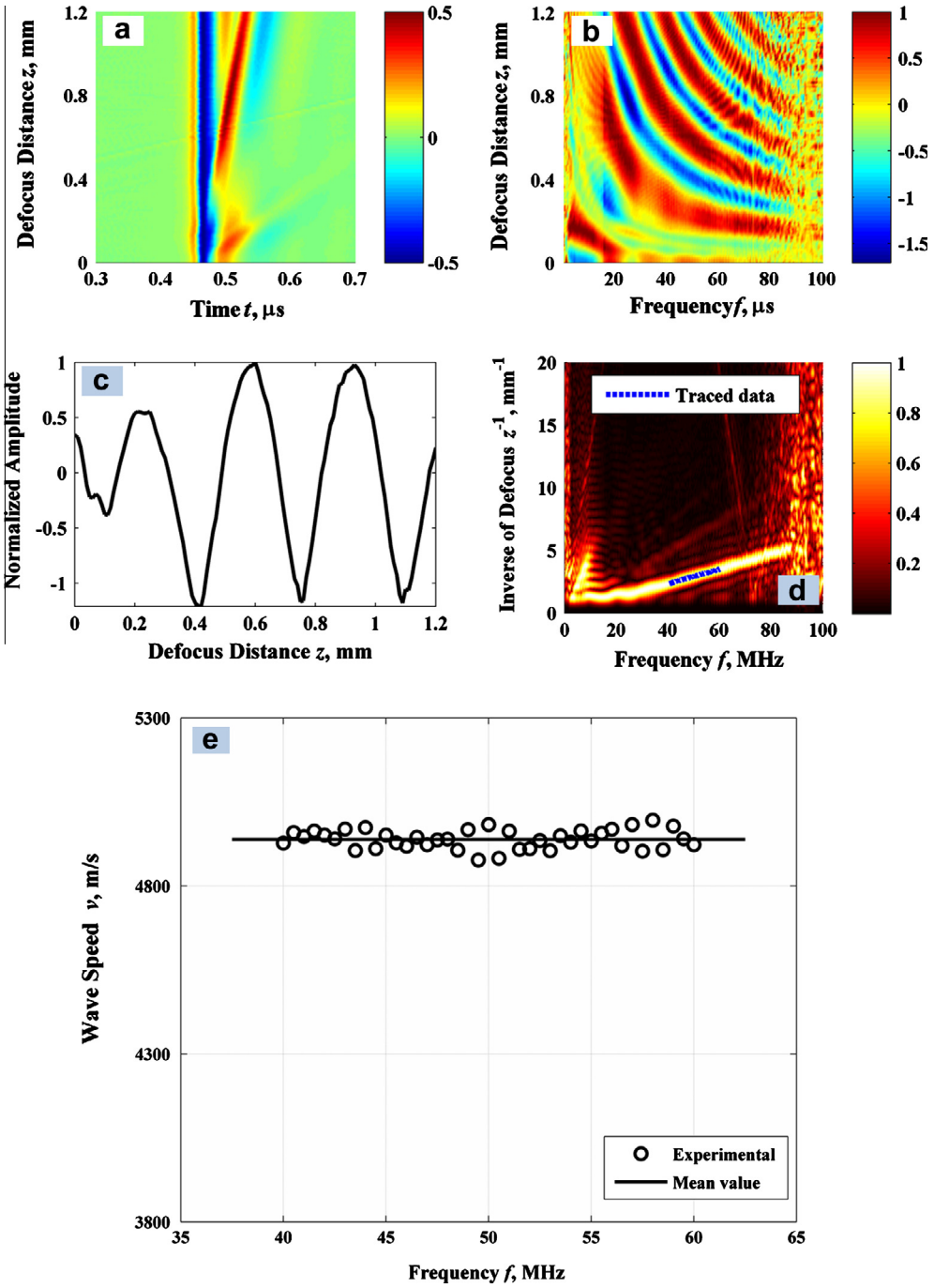

Fig. 8. Progressive defocusing measurements of a 500 μm (100) silicon wafer at [100]+10.5°: (a) time domain waveforms; (b) Fourier transform with respect to t; (c) $V(f,z)$ curve at 50 MHz; (d) Image representation of Fourier transform of $V(f,z)$ data with respect to z; and (e) measured surface wave speed.

Firstly, the normalized time domain waveforms $A(t,z)$, as shown in Fig. 8(a), are Fourier transformed with respect to time t into frequency domain f, hereinafter referred to as $V(f,z)$ data shown in Fig. 8(b). The oscillating $V(f,z)$ curve at a certain frequency of 50 MHz is very similar to the conventional $V(z)$ curve in AM, as shown in Fig. 8(c). As a matter of fact, they both are induced by the interference between the directly reflected ray #1 and the surface wave mode ray #2. Secondly, in order to determine the oscillating period Δz in $V(f,z)$ curve accurately, the $V(f,z)$ data are Fourier transformed to wave number k domain (actually it's the inverse of z) with respect to z, referred to as $V'(f,k)$ data shown in Fig. 8(d). The oscillating period Δz will be determined by tracing the maxima on the "ridge", and it can be observed that the tracing range can extend from several MHz to over 90 MHz. Once the Δz is determined, the SAW velocities will be obtained by Eq. (2), as shown in Fig. 8(e). It appears that the velocities are very close to a constant from 40 MHz to 60 MHz with a discrepancy of less than 100 m/s. Now we can use the mean value of 4938 m/s to represent the SAW velocity at [100]+10.5°.

Applying the processing method to each series of waveforms from different azimuthal directions, the final SAW velocities versus directions will be acquired, as shown in Fig. 9. The theoretical results are calculated through the partial wave method reported in Ref. [32] using the parameters in Ref. [35]. Here it should be

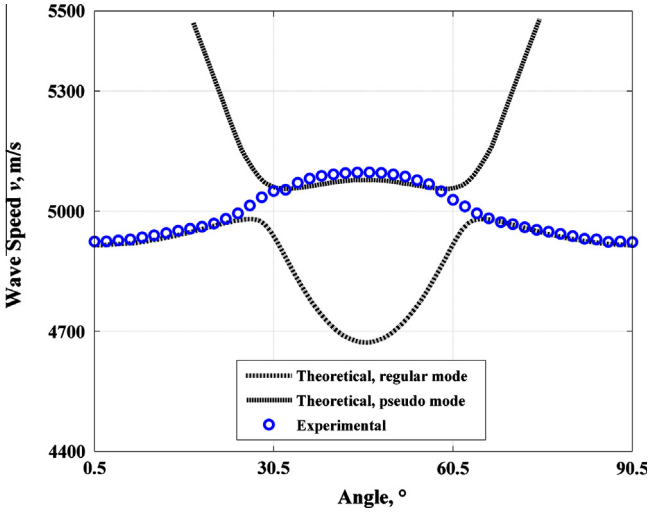

Fig. 9. Experimental and theoretical velocities with respect to all the azimuthal angle between [100]+0.5° and [010]+0.5° direction.

mentioned that because the mass density of the silicon is much greater than that of water, the difference between SAW velocities and leaky SAW velocities can be neglected [36]. Hence, a vacuum/solid model will replace the water/solid model. Finally, the corresponding measurement average velocity error throughout all the directions is below 1%.

4. Conclusions and discussion

A broadband P(VDF-TrFE) line-focus ultrasonic transducer (LT1) with high center frequency of 60 MHz, large aperture angle of 90° and −6 dB bandwidth of 50 MHz is successfully fabricated through the improved "spin-coating thermal-crystallization simultaneously" method which is specially applicable and reliable for line-focus transducers. To analyze the piezoelectric properties of P(VDF-TrFE) films achieved from different VDF/TrFE molar ratio, ferroelectric hysteresis loops are measured to select the better parameters. Also, the strategy of poling the films is addressed. A conventional transducer (LT2) is fabricated for comparison, and the focal plane response indicates that the LT1 shows better performance: larger peak-to-peak value, higher center frequency, relatively wider bandwidth (−6 dB). According to our experience, at this scale of aperture angle and focal radius, higher center frequency transducers are difficult to obtain. This may be due to the attenuation of coupling water and the elastic vibrating abilities at resonant frequency.

Different types of samples can be used as the target of this line-focus transducer, including isotropic and specially anisotropic materials. Moreover, the broadband properties enable the dispersion curves measurement of thin plates. In this paper, a typical (100) silicon wafer is measured along various directions between [100] and [010] in a 2° incremental step to represent the anisotropic features. The V(f,z) processing method allows a continuous wave velocities extraction and exhibits an easy way for defocusing measurement data analysis. Finally, the measured anisotropic surface wave velocities demonstrate a good agreement with the theoretical predictions.

Acknowledgments

The work presented in this paper is supported by the National Natural Science Foundation of China (Nos. 11172014, 51235001 and 61271372), the National Research Foundation for the Doctoral Program of Higher Education of China (No. 20091103110004), and Beijing City Board of Education Science and Technology Plan (No. KM201010005034).

References

[1] A. Neubrand, P. Hess, Laser generation and detection of surface acoustic-waves – elastic properties of surface-layers, J. Appl. Phys. 71 (1992) 227–238.
[2] P. Hess, Laser diagnostics of mechanical and elastic properties of silicon and carbon films, Appl. Surf. Sci. 106 (1996) 429–437.
[3] T.T. Wu, Y.H. Liu, On the measurement of anisotropic elastic constants of fiber-reinforced composite plate using ultrasonic bulk wave and laser generated Lamb wave, Ultrasonics 37 (1999) 405–412.
[4] R.A. Lemons, C.F. Quate, Acoustic microscope – scanning version, Appl. Phys. Lett. 24 (1974) 163–165.
[5] A. Atalar, C.F. Quate, H.K. Wickramasinghe, Phase imaging in reflection with the acoustic microscope, Appl. Phys. Lett. 31 (1977) 791–793.
[6] R.D. Weglein, R.G. Wilson, Characteristic material signatures by acoustic microscopy, Electron. Lett. 14 (1978) 352–354.
[7] W. Parmon, H.L. Bertoni, Ray interpretation of the material signature in the acoustic microscope, Electron. Lett. 15 (1979) 684–686.
[8] J. Kushibiki, N. Chubachi, Material characterization by line-focus-beam acoustic microscope, IEEE Trans. Sonics Ultrason. 32 (1985) 189–212.
[9] Y.C. Lee, Y.F. Tein, Y.Y. Chao, A point-focus PVDF transducer for Lamb wave measurements, Chin. J. Mech.-Ser. A 18 (2002) 29–33.
[10] S. Smolorz, W. Grill, Focusing PVDF transducers for acoustic microscopy, Res. Nondestruct. Eval. 7 (1996) 195–201.
[11] D. Xiang, N.N. Hsu, G.V. Blessing, The design, construction and application of a large aperture lens-less line-focus PVDF transducer, Ultrasonics 34 (1996) 641–647.
[12] N.N. Hsu, D. Xiang, G.V. Blessing, Time-resolved ultrasonic body wave measurements of material anisotropy using a lensless line-focus transducer, 1998 Ieee Ultrasonics Symposium – Proceedings, vols. 1 and 2, 1998, pp.1261–1264.
[13] Y.-C. Lee, J.O. Kim, J.D. Achenbach, Measurement of stresses by line-focus acoustic microscopy, Ultrasonics 32 (1994) 359–365.
[14] J. Kushibiki, T. Sannomiya, N. Chubachi, Broad bandwidth concave transducer for scanning acoustic microscope, Electron. Lett. 17 (1981) 42–44.
[15] N. Chubachi, J. Kushibiki, T. Sannomiya, Y. Iyama, Performance of scanning acoustic microscope employing concave transducers, IEEE Trans. Sonics Ultrason. 27 (1980). 152–152.
[16] Y.-C. Lee, Y.F. Tein, Y.Y. Chao, A point-focus PVDF transducer for lamb wave measurements, Chin. J. Mech. Ser. A (English Edition) 18 (2002) 29–33.
[17] Y.-C. Lee, C.-C. Chu, A double-layered line-focusing PVDF transducer and V(z) measurement of surface acoustic wave, Jap. J. Appl. Phys., Part 1: Regular Papers and Short Notes and Review Papers 44 (2005) 1462–1467.
[18] K. Kimura, H. Ohigashi, Generation of very high-frequency ultrasonic-waves using thin-films of vinylidene fluoride-trifluoroethylene copolymer, J. Appl. Phys. 61 (1987) 4749–4754.
[19] M. Robert, G. Molingou, K. Snook, J. Cannata, K.K. Shung, Fabrication of focused poly(vinylidene fluoride-trifluoroethylene) P(VDF-TrFE) copolymer 40–50 MHz ultrasound transducers on curved surfaces, J. Appl. Phys. 96 (2004) 252–256.
[20] K. Snook, S. Rhee, M. Robert, E. Gottlieb, K.K. Shung, Development of P(VDF-TRFE) ultrasonic transducers operating at 50-120 MHz, in: 2002 IEEE Ultrasonics Symposium, October 8, 2002–October 11, 2002, Institute of Electrical and Electronics Engineers Inc., Munich, Germany, 2002, pp. 1249–1252.
[21] C.-H. Chung, Y.-C. Lee, Fabrication of poly(vinylidene fluoride-trifluoroethylene) ultrasound focusing transducers and measurements of elastic constants of thin plates, NDT E Int. 43 (2010) 96–105.
[22] Y.-C. Lee, Measurements of dispersion curves of leaky Lamb waves using a lens-less line-focus transducer, Ultrasonics 39 (2001) 297–306.
[23] C.-H. Chung, Y.-C. Lee, Nondestructive determination of elastic constants of thin isotropic plates based on poly(vinylidene fluoride-trifluoroethylene) copolymer ultrasound focusing transducers and lamb wave measurements, Jpn. J. Appl. Phys. 48 (2009).
[24] C.-H. Chung, Y.-C. Lee, Broadband poly(vinylidene fluoride-trifluoroethylene) ultrasound focusing transducers for determining elastic constants of coating materials, J. Nondestruct. Eval. 28 (2009) 101–110.
[25] Y.-C. Lee, S.H. Kuo, Double-layer PVDF transducer and V(z) measurement system for measuring leaky Lamb waves in a piezoelectric plate, Ultrasonics 46 (2007) 25–33.
[26] H.L. Bertoni, Ray-optical evaluation of V(z) in the reflection acoustic microscope, Sonics Ultrasonics, IEEE Trans. 31 (1984) 105–116.
[27] P. Mutti, A. Briggs, D. Bowler, Oscillations in V(z) curves of thin samples, Ultrasonics, Ferroelectrics Freq Control, IEEE Trans. 42 (1995) 567–570.
[28] C.-H. Yang, Characterization of Piezoelectrics Using Line Focus Transducer, in: Proceedings of 15th Conference of Chinese Society of Mechanical Engineering, 1998, pp. 785–790.
[29] J. Kushibiki, K. Horii, N. Chubachi, Velocity measurement of multiple leaky waves on germanium by line-focus-beam acoustic microscope using FFT, Electron. Lett. 19 (1983) 404–405.

[30] J. Kushibiki, K. Horii, N. Chubachi, FFT velocity measurement of multiple leaky waves by line-focus-beam acoustic microscope, in, Ultrason. Symp. 1983 (1983) 637–640.
[31] D. Alleyne, P. Cawley, A two-dimensional Fourier transform method for the measurement of propagating multimode signals, J. Acoust. Soc. Am. 89 (1991) 1159–1168.
[32] A.H. Nayfeh, Wave propagation in layered anisotropic media: with applications to composites, North Holland, 1995.
[33] T. Furukawa, Structure and functional properties of ferroelectric polymers, Adv. Colloid Interface 71–2 (1997) 183–208.
[34] Y.-C. Lee, S.-P. Ko, Measuring dispersion curves of acoustic waves using PVDF line-focus transducers, NDT E Int. 34 (2001) 191–197.
[35] T. Kundu, Ultrasonic Nondestructive Evaluation: Engineering and Biological Material Characterization, CRC, 2004.
[36] I.A. Viktorov, Rayleigh and Lamb Waves: Physical Theory and Applications, Plenum press, New York, 1967.